THE JOURNAL OF BIOLOGICAL CHEMISTRY
Vol. 276, No. 48, Issue of November 30, pp. 45236–45242, 2001
Printed in U.S.A.

Phospholipase Cβ4 and Protein Kinase Cα and/or Protein Kinase CβI Are Involved in the Induction of Long Term Depression in Cerebellar Purkinje Cells*

Received for publication, June 12, 2001, and in revised form, August 30, 2001
Published, JBC Papers in Press, September 10, 2001, DOI 10.1074/jbc.M105413200

Moritoshi Hirono‡§, Takashi Sugiyama§¶, Yasushi Kishimoto‖, Ikuko Sakai, Takahito Miyazawa‡‡, Masahiro Kishio¶, Hiroko Inoue¶, Kazuki Nakao§§, Masayuki Ikeda‡, Shigenori Kawahara‖, Yutaka Kirino‖, Motoya Katsuki§§, Hidenori Horie**, Yoshihiro Ishikawa**, and Tohru Yoshioka‡¶ ¶¶**

*From the ‡Department of Molecular Neurobiology, Advanced Research Institute for Science and Engineering, Waseda University, 3-4-1 Okubo, Shinjuku-ku, Tokyo 169-8555, the ¶Department of Molecular Neurobiology, School of Human Sciences, Waseda University, 2-579-15 Mikajima, Tokorozawa-shi, Saitama 359-1192, the ‖Laboratory of Neurobiophysics, School of Pharmaceutical Sciences, The University of Tokyo, 7-3-1 Hongo, Bunkyo-ku, Tokyo 113-0033, the **Department of Physiology, School of Medicine, Yokohama City University, 3-9 Fuku-ura, Kanazawa-ku, Yokohama 236-0004, the ‡‡Department of Neurosurgery, National Defense Medical College, 3-2 Namiki, Tokorozawa-shi, Saitama 359-8513, the §§Department of DNA Biology and Embryo Engineering, Research Center of Animal Models for Human Diseases, The Institute of Medical Science, The University of Tokyo, 4-6-1 Shirokanedai, Minato-ku, Tokyo 108-8639, Japan*

Activation of the type-1 metabotropic glutamate receptor (mGluR1) signaling pathway in the cerebellum involves activation of phospholipase C (PLC) and protein kinase C (PKC) for the induction of cerebellar long term depression (LTD). The PLC and PKC isoforms that are involved in LTD remain unclear, however. One previous study found no change in LTD in PKCγ-deficient mice, thus, in the present study, we examined cerebellar LTD in PLCβ4-deficient mice. Immunohistochemical and Western blot analyses of cerebellum from wild-type mice revealed that PLCβ1 was expressed weakly and uniformly, PLCβ2 was not detected, PLCβ3 was expressed predominantly in caudal cerebellum (lobes 7–10), and PLCβ4 was expressed uniformly throughout. In PLCβ4-deficient mice, expression of total PLCβ, the mGluR1-mediated Ca^{2+} response, and LTD induction were greatly reduced in rostral cerebellum (lobes 1–6). Furthermore, we used immunohistochemistry to localize PKCα, -βI, -βII, and -γ in mouse cerebellar Purkinje cells during LTD induction. Both PKCα and PKCβI were found to be translocated to the plasmamembrane under these conditions. Taken together, these results suggest that mGluR1-mediated activation of PLCβ4 in rostral cerebellar Purkinje cells induced LTD via PKCα and/or PKCβI.

Cerebellar long term depression (LTD)[1] is produced by associative activation of parallel fiber (PF) and climbing fiber synapses (1–4), which results in co-activation of α-amino-3-hydroxy-5-methyl-4-isoxazolepropionic acid receptors (AMPAR) and type-1 metabotropic glutamate receptors (mGluR1) in Purkinje cells followed by activation of phospholipase C (PLC) coupled to G_q, hydrolysis of phosphatidylinositol 4,5-bisphosphate (PIP_2) to inositol 1,4,5-trisphosphate (IP_3) and diacylglycerol, an increase in the concentration of intracellular Ca^{2+} ($[Ca^{2+}]_i$), and activation of protein kinase C (PKC; for review, see Ref. 5).

As predicted, mGluR1-deficient mutant mice exhibit impaired cerebellar LTD (6, 7), however, there is no disruption of LTD in PKCγ-deficient mice (8). These results raise the possibility that disruption of one of the intermediate molecules in the mGluR1 signaling pathway may disrupt LTD. Of the four isoforms of PLC, PLCβ1–4 (9, 10), two are abundant in the cerebellum, PLCβ3 and PLCβ4 (11–13). PLCβ3 is expressed predominantly in the caudal half of cerebellar Purkinje cells, whereas PLCβ4 is distributed throughout cerebellar Purkinje cells. Fly homologue of PLCβ4 has been implicated in transduction of visual information in *Drosophila* photoreceptors (14, 15), however, the role of PLCβ4 in the cerebellum remains unknown. The PLCβ4-deficient mice were viable but had a higher mortality rate than wild-type mice, and the body weight of PLCβ4-deficient mice was generally less than that of wild-type mice in the early stages of postnatal development, as reported previously (16, 17). The body weight of the PLCβ4-deficient mice gradually increased to match wild-type mice 8 weeks after birth. Using a light microscope, no differences were detected in the size of whole cerebellum, lobe size, or Purkinje cell size between PLCβ4-deficient and wild-type mice. Anatomical alterations are minimal in mGluR1-deficient mutant mice (6) and cerebellar architecture is also normal in glial fibrillary acidic protein (GFAP)-deficient mutant mice (18). Only one abnormality in the cerebellar anatomy of PLCβ4-deficient mice

* This work was supported by a Grant-in-Aid (0727910 to T. Y.) for Scientific Research on Priority Areas on "Functional Development of Neural Circuits" from the Ministry of Education, Science, Sports and Culture of Japan; by Research for the Future Program (96L00310 to T. Y.); a Grant-in-Aid (12780603 to M. H.) for Encouragement of Young Scientists from Japan Society for the Promotion of Science; and by a grant from the Program for Promotion of Basic Research Activity for Innovative Bioscience. The costs of publication of this article were defrayed in part by the payment of page charges. This article must therefore be hereby marked "*advertisement*" in accordance with 18 U.S.C. Section 1734 solely to indicate this fact.

§ These authors contributed equally to this work.
¶¶ To whom correspondence should be addressed: Tel./Fax: 81-3-3205-6419; E-mail: yoshioka@human.waseda.ac.jp.

[1] The abbreviations used are: LTD, long term depression; PF, parallel fiber; AMPA, α-amino-3-hydroxy-5-methyl-4-isoxazolepropionic acid; mGluR, metabotropic glutamate receptor; PLC, phospholipase C; PIP_2, phosphatidylinositol 4,5-bisphosphate; IP_3, inositol 1,4,5-trisphosphate; $[Ca^{2+}]_i$, intracellular Ca^{2+}; PKC, protein kinase C; ACSF, artificial cerebrospinal fluid; EPSC, excitatory postsynaptic current; GABA, γ-aminobutyric acid; GFAP, glial fibrillary acidic protein; CJ, conjunctive stimulation protocol; DHPG, (*RS*)-3,5-dihydroxyphenylglycine; TPA, 12-*O*-tetradecanoylphorbol-13-acetate.

has been reported so far; persistent multiple climbing fiber innervation of Purkinje cells (19), which has also been reported in mGluR1-, GluRδ2-, and PKCγ-deficient but not GFAP-deficient mice (18, 20–22). Eight PKC isozymes (α, βI, βII, γ, δ, ϵ, ζ, and η) are expressed in the cerebellum, of which six (α, βI, γ, δ, ϵ, and ζ) are found in cerebellar Purkinje cells (23–25). Selective expression of a pseudosubstrate PKC inhibitor, PKC inhibitor peptide (Arg^{19}-Val^{31}), in Purkinje cells completely blocked cerebellar LTD (26). Therefore, using PLCβ4-deficient mice in the present study, we examined the effects of disruption of PLCβ4 on cerebellar LTD and determined which PKC isozymes were essential for the induction of LTD.

EXPERIMENTAL PROCEDURES

Generation of PLCβ4-deficient Mice—Mice with a disruption of the PLCβ4 gene were generated in the laboratory of M. Katsuki according to standard methods (27). A genomic clone encoding the PLCβ4 catalytic region (denoted the Y region) was isolated to construct a targeting vector in which exons that encode amino acid residues 539–646 were replaced with a neomycin-resistant gene cassette, and a diphtheria toxin fragment A gene was attached to the 3′-end of the targeting vector for negative selection. Embryonic stem cells were transfected with the targeting vector by electroporation and selected with G418 (250 μg/ml) for 8 days. G418-resistant colonies were isolated, and the targeted clones were selected using genomic Southern blot analysis with a probe as illustrated in Fig. 1*A*. Chimeric mice were generated from frozen C57BL/6J blastocytes injected with the embryonic stem cells after warming (28). Male chimeric mice were mated with C57BL/6J female mice. The tail DNA of offspring was analyzed using Southern blot analysis (Fig. 1*B*) to identify the genotype or amplified using polymerase chain reaction.

Phospholipase C Assay—PLC enzymatic activity was quantified in 200 μl of assay mixture containing 150 μM PIP_2. The mixture contained 20,000 cpm [^{3}H]PIP_2, 1 mM EGTA, 10 mM $CaCl_2$, 0.1% sodium deoxycholate, 1 mg/ml bovine serum albumin, and 50 mM HEPES, pH 6.8. The reaction mixture was incubated at 37 °C and centrifuged (10,000 × *g* for 30 min) to precipitate the cerebellar homogenate, and the reaction was terminated as previously described (29).

Western Blot Analysis and Immunohistochemistry—Each lobe of the vermis of the cerebellum from wild-type and PLCβ4-deficient mice was homogenized, and 3 μg of protein was separated using 7.5% SDS-polyacrylamide gel electrophoresis. Separated proteins were transferred to a nitrocellulose membrane. The membrane was incubated with anti-PLCβ1, -β2, -β3, or -β4 antibodies (1/1000 dilution, Santa Cruz Biotechnology, Santa Cruz, CA) and then with an alkaline-phosphatase-labeled secondary antibody (1/5000 dilution, Promega, Madison, WI). Immunoreacted bands were visualized using ProtoBlot Western blot AP Systems (Promega).

At the third or fourth postnatal week, mice were deeply anesthetized with pentobarbital (4 mg/100 g) and transcardially perfused with 4% phosphate-buffered paraformaldehyde (4 °C, pH 7.4). The brains were immersed in the same fixative for half a day and then embedded in paraffin. Sagittal or coronal paraffin-embedded sections (3–5 μm thick) were prepared for immunohistochemical visualization using a streptavidin-peroxidase reaction (Nichirei Co. Ltd., Japan (30, 31)). As a blocking step, the sections were incubated with 3% H_2O_2 in distilled water for 10 min and then 10% normal goat serum for 1 h. Affinity-purified rabbit polyclonal primary antibodies against either mouse PLCβ3 (1/500), PLCβ4 (1/50), PKCα (1/100, Life Technologies, Inc., Rockville, MD), PKCβI (1/500, Life Technologies, Inc.), PKCβII (1/500, Life Technologies, Inc.), or PKCγ (1/500, Life Technologies, Inc.) were applied to brain sections overnight at 4 °C. Subsequently, sections were incubated with biotin-conjugated goat anti-rabbit immunoglobulin G for 1 h at room temperature (23–26 °C). Sections were then incubated with peroxidase-conjugated streptavidin for 1 h at room temperature. Between each incubation step, the sections were rinsed twice in 0.01 M phosphate-buffered saline, pH 7.4, for 5 min each. The final peroxidase reaction was performed using 0.05% diaminobenzidine and 0.005% H_2O_2. The same sections were stained with cresyl violet for Nissl staining. For immunohistochemical analysis of PKC isozymes, a fluorescein isothiocyanate-conjugated secondary antibody was used and the immunostained sections were examined using fluorescence microscopy.

Ca^{2+} Imaging—Sagittal slices (180–200 μm thick) of cerebellar vermis were prepared from 3- to 5-week-old wild-type and PLCβ4-deficient mice using a microslicer (DTK-1000, Dosaka, Japan) and maintained at room temperature in artificial cerebrospinal fluid (ACSF), which consisted of 138.6 mM NaCl, 3.35 mM KCl, 21 mM $NaHCO_3$, 0.6 mM NaH_2PO_4, 9.9 mM glucose, 2.5 mM $CaCl_2$, and 1 mM $MgCl_2$ and was gassed with a mixture of 95% O_2 and 5% CO_2 (pH 7.4). The Ca^{2+} indicator fura-2 (1 mM, Dojin, Japan) was injected into Purkinje cells for 25–45 min through patch pipettes or cerebellar slices were incubated in 10 μM fura-2 AM (Dojin) for 1 h with 0.001% Cremophore EL. The slices were then maintained in ACSF for at least 30 min and transferred to the stage of an Axioplan 2 microscope (Zeiss, Germany). Fluorescence Ca^{2+} ratio imaging was carried out by excitation of the indicator at 340:380 nm, and paired emission images were acquired using a cooled charge-coupled device camera (C4880, Hamamatsu Photonics, Japan) at 510 nm. Fluorescence images were acquired using a 60× water immersion objective (LUMPlanFI, numerical aperture (NA) 0.90, Olympus, Japan) that efficiently passed 340-nm light, and ratios were determined using a digital image acquisition system and image-processing software (ARGUS 50/CA, Hamamatsu Photonics, Japan).

Electrophysiology—Whole-cell voltage-clamp recordings were made from visually identified Purkinje cells under Nomarski optics using a 40× water immersion objective (NA 0.75, Zeiss). Patch pipettes (3–4 MΩ) were filled with intracellular solution containing 150 mM KCH_3SO_3, 5 mM KCl, 0.3 mM K-EGTA, 5.0 mM sodium HEPES, 3.0 mM Mg-ATP, and 0.4 mM Na-GTP (pH 7.4). Membrane currents were recorded using an EPC-7 amplifier (List Electronics, Darmstadt, Germany) and pCLAMP software (Axon Instruments, Union City, CA), digitized, and stored on a computer disc for off-line analysis. PF-mediated ionotropic-glutamate-receptor-type excitatory postsynaptic currents (EPSCs) were identified based on response properties following paired-pulse stimulation (duration, 50–100 μs; amplitude, 5–15 V) applied via a glass microelectrode with 2- to 3-μm tip diameter, filled with normal ACSF, and placed within the molecular layer in the cerebellar cortex. Paired-pulse stimulation was applied at 0.2 Hz. For measuring PF-evoked EPSCs, bicuculline (10 μM) was added to the ACSF to eliminate γ-aminobutyric acid (GABA)-mediated postsynaptic currents. Series resistance (8–18 MΩ) was monitored using a −5-mV hyperpolarizing voltage step after PF stimulation. The series resistance compensation control of the amplitude was set between 60 and 70%. mGluR1-mediated EPSCs were obtained using repetitive, high frequency stimulation (10 pulses at 100 Hz; duration, 180 μs; amplitude, 30 V). To prevent ionotropic glutamate and $GABA_A$ receptor responses, 6-cyano-7-nitroquinoxaline-2,3-dione (10 μM), D(−)-2-amino-5-phosphonopentanoic acid (30 μM), and bicuculline (50 μM) were added to the external solution. All physiological experiments were performed at room temperature.

Pharmacological Stimulation—The experimental protocols for LTD were performed as described previously with slight modification (32, 33). Briefly, sagittal slices (400 μm thick) of cerebellar vermis were prepared from 3- to 5-week-old wild-type and PLCβ4-deficient mice using a microslicer and maintained at room temperature in ACSF, including 0.5 μM tetrodotoxin and 1 μM BAPTA-AM, and saturated with 95% O_2/5% CO_2. To stimulate the cells, each slice was then transferred to a cylinder chamber (ϕ 35 mm) in medium containing 50 mM KCl and 100 μM glutamate. Five minutes after stimulation, the slices were washed with ACSF for 5 min, followed by fixation with 4% paraformaldehyde. Immunohistochemistry was performed as described under "Western Blot Analysis and Immunohistochemistry."

Statistics—Data were analyzed using one-way analysis of variance, and statistical significance was determined using a Student's *t* test or Mann-Whitney *U* test. Differences were considered significant when *P* was less than 0.05.

During the course of the present study, the care of the animals conformed to the guidelines established by the Institutional Animal Investigation Committee at the University of Tokyo.

RESULTS

Biochemical and Histological Characterization of Cerebellar PLCβ—The total activity of membrane-associated PLC was examined using [^{3}H]PIP_2 as a substrate in cerebellar slices from wild-type (n = 4) and PLCβ4-deficient mice (n = 5). As shown in Fig. 1*C*, the total PLC activity in PLCβ4-deficient mice was less than 30% of control values in rostral cerebellum and less than 40% in caudal cerebellum. These data suggest that PLCβ4 activity in rostral and caudal cerebellum was 70 and 60% of the total PLC activity, respectively. Total PLC activity was found to be 5.6 nmol/mg/min in rostral cerebellum and 4.5 nmol/mg/min in caudal cerebellum.

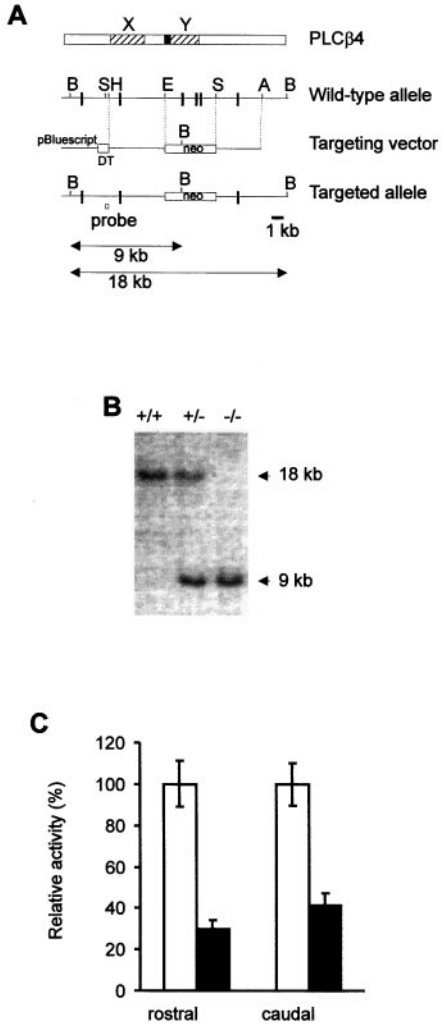

FIG. 1. **Generation of PLCβ4-deficient mice.** *A*, the targeting vector and the homologous recombination process are shown. The *black box* represents the targeted exon; the *white box* under the mutant allele indicates the probe used for Southern blot analysis; *A*, *Apa*I; *B*, *Bam*HI; *E*, *Eco*RI; *H*, *Hin*dIII; *S*, *Sac*I; *DT*, diphtheria toxin A fragment; *neo*, neomycin-resistant gene cassette. *B*, Southern blot analysis for genotyping. Tail DNA was isolated, digested with *Bam*HI, and separated using gel electrophoresis. The DNA was transferred to nylon membranes and hybridized with the probe indicated in *A*. The 18-kb band was the wild-type allele, and the 9-kb band was the targeted allele. *C*, PLC activity in rostral and caudal cerebellum from wild-type ($n = 4$; *open bars*) and PLCβ4-deficient mice ($n = 5$; *solid bars*) was assayed for PIP_2 hydrolysis. *Bars* represent mean ± S.E.

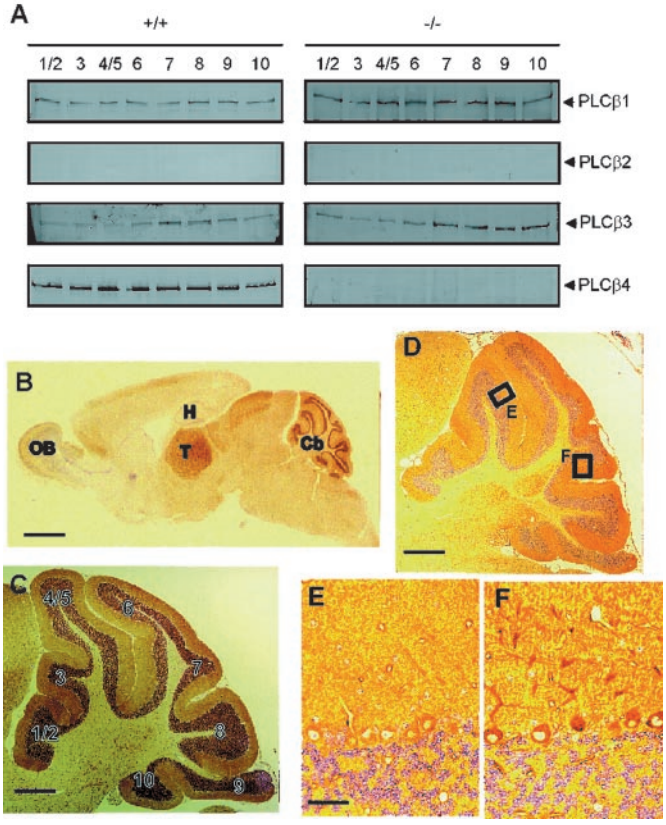

FIG. 2. *A*, Western blot of cerebellar proteins from wild-type (+/+) and PLCβ4-deficient mice (−/−). The PLCβ1 and -β4 isoforms were expressed evenly throughout the cerebellum of wild-type mice, and PLCβ3 was observed primarily in caudal (*lobes 7–10*) cerebellum. PLCβ2 was not detected. *B–F*, immunohistochemical analyses of whole-brain and cerebellar sections. The whole-brain and cerebellar sections from wild-type mice were immunostained with anti-PLCβ4 (*B* and *C*) or anti-PLCβ3 (*D–F*) antibodies. Hippocampus did not immunoreact with anti-PLCβ4 antibody (*B*). The lobes of mouse cerebellum were numbered *1–10* as indicated (*C*). *E*, a higher power view of the rostral cerebellum (*lobes 4* and *5*) indicated by *box E* in *D*. Purkinje cells exhibited weak PLCβ3 immunoreactivity. *F*, a higher power view of the caudal cerebellum (*lobe 7*) indicated by *box F* in *D*, showing strong PLCβ3 immunoreactivity in dendrites and cell bodies of Purkinje cells. *Cb*, cerebellum; *H*, hippocampus; *OB*, olfactory bulb; *T*, thalamus. *Scale bars*: 1 mm in *B*, 500 μm in *C* and *D*, and 70 μm in *E* and *F*.

Western blot analysis (Fig. 2*A*) indicates that PLCβ1, PLCβ3, and PLCβ4 were expressed in wild-type mouse cerebellum. PLCβ4 protein was not detected in the cerebellum from PLCβ4-deficient mice (Fig. 2*A*), whereas the expression levels of the other PLCβ isoforms (PLCβ1, PLCβ2, and PLCβ3) were not altered.

Immunohistochemical analysis was performed using an anti-PLCβ4 antibody (Fig. 2, *B* and *C*). Each of the lobes in the cerebellar slices was numbered from 1 to 10 as shown in Fig. 2*C*. PLCβ4 was expressed uniformly in Purkinje cells in rostral (*lobes 1–6*) and caudal (*lobes 7–10*) cerebellum from wild-type mice (Fig. 2*C*), whereas PLCβ3 is more abundant in Purkinje cells in caudal cerebellum from wild-type mice (13, 19; Fig. 2, *D–F*). No morphological changes were observed in the cerebellum of PLCβ4-deficient mice when examined using light microscopy (data not shown).

Normal PF-Purkinje Cell Synaptic Transmission in PLCβ4-deficient Mouse Cerebellum—To examine PF-Purkinje cell synaptic function in PLCβ4-deficient mice, we measured the rise and decay time constants of EPSCs, which were calculated using a single-exponential fit (34) and paired-pulse facilitation in acute cerebellar slices. The mean rise time constant was 1.23 ± 0.06 ms ($n = 30$) and 1.21 ± 0.05 ms ($n = 35$) in Purkinje cells from wild-type and PLCβ4-deficient mice, respectively. The mean decay time constant was 14.1 ± 0.5 ms ($n = 30$) in wild-type *versus* 12.8 ± 0.5 ms ($n = 35$) in PLCβ4-deficient Purkinje cells. There was no significant difference in either the rise or decay time constants between wild-type and PLCβ4-deficient mice ($p > 0.05$; Fig. 3, *A* and *B*). The PF responses exhibited paired-pulse facilitation (35), which decreased with increasing interpulse intervals in a similar manner in wild-type and PLCβ4-deficient mice (Fig. 3*C*). Therefore, short term plasticity in PF-Purkinje cell synapses appeared normal in PLCβ4-deficient mice. Furthermore, no significant difference was found in the resting membrane potentials (−55.5 ± 1.3 mV *versus* −56.3 ± 1.5 mV) of Purkinje cells from wild-type and PLCβ4-deficient mice.

LTD Was Not Inducible in Rostral Cerebellum from PLCβ4-deficient Mice—LTD of synaptic transmission at PF-Purkinje cell synapses is induced by simultaneous low frequency activation of PF and climbing fibers (1, 3). Climbing fiber stimulation

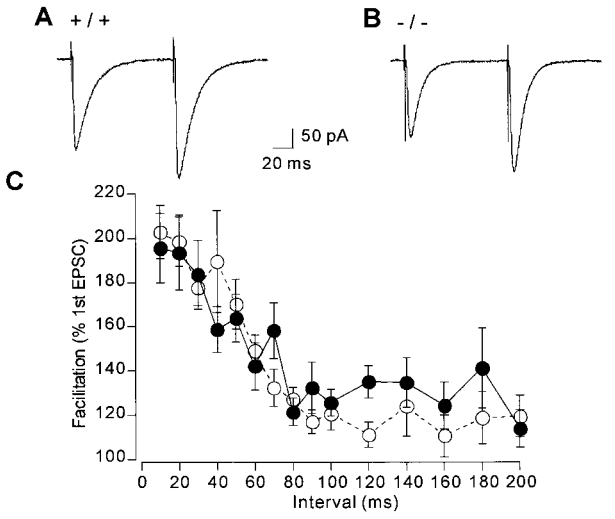

FIG. 3. **The mean rise and decay times and paired-pulse facilitation of Purkinje cell synaptic responses were not affected in PLCβ4-deficient mice.** *A–C*, PF-EPSCs were unaltered in Purkinje cells from PLCβ4-deficient mice. Representative traces showing the response to paired-pulse stimulation in a Purkinje cell from a wild-type mouse (*A*) and a PLCβ4-deficient mouse (*B*). Each *trace* is the average of 12 consecutive EPSCs. The holding potential was −60 mV. *C*, paired-pulse facilitation of PF-EPSCs (expressed as the ratio of the responses to the first and second pulses) in Purkinje cells from wild-type (*open circle*; $n = 10$, from six mice) and PLCβ4-deficient (*solid circle*; $n = 12$, from six mice) mice is plotted as a function of interpulse interval. Data points represent the mean ± S.E.

can be replaced by depolarizing Purkinje cells to allow calcium influx through voltage-gated calcium channels (36, 37). We recorded PF-EPSCs from Purkinje cells in cerebellar lobes from wild-type and PLCβ4-deficient mice using whole-cell patch clamp and a conjunctive stimulation protocol (CJ) composed of 300 PF stimuli in conjunction with a depolarizing pulse (200 ms, −60 to +20 mV) repeated at 1 Hz. In 21 of 25 Purkinje cells from wild-type mice (*lobes 1–10*), CJ stimulation depressed the amplitude of PF-EPSCs, and this depression persisted over 30 min after the onset of the stimulation (Fig. 4*A*). The mean PF-EPSCs amplitude, measured 25–30 min after CJ stimulation, was reduced to 75.8% ± 3.6% ($n = 17$ from 13 mice, two cells studied blind) of the original baseline EPSC amplitude. Depression could be induced even after 40 min in whole-cell recording configuration, indicating that cell dialysis had no significant effect on LTD induction. In PLCβ4-deficient mice, Purkinje cells exhibited reduced LTD after CJ stimulation in rostral cerebellum (*lobes 1–6*; Fig. 4*B*), whereas LTD was intact in caudal cerebellum (*lobes 7–10*; Fig. 4*C*). The mean amplitude of PF-EPSCs in rostral cerebellum recorded 25–30 min after CJ stimulation was 90.1% ± 5.5% of control ($n = 16$ from 11 mice, two cells studied blind). The difference between the wild-type and PLCβ4-deficient mice was significant (Mann-Whitney *U* test, $p < 0.05$) in rostral cerebellum, whereas LTD from caudal cerebellum in PLCβ4-deficient mice (67.5% ± 2.5%; $n = 11$ from 10 mice) was comparable to LTD in wild-type mice (Mann-Whitney *U* test, $p > 0.05$).

Determination of the PKC Isozymes Activated by PLCβ4—PKC isozymes in Purkinje cells from PLCβ4-deficient mice were examined as a function of mGluR1-mediated IP_3-dependent Ca^{2+} mobilization. Only classic PKC isozymes (α, βI, βII, and γ) can be activated by IP_3-activated Ca^{2+} release and diacylglycerol (38). Although application of the mGluR1-specific agonist (*RS*)-3,5-dihydroxyphenylglycine (DHPG) has been shown to increase $[Ca^{2+}]_i$ in rodent cerebellar Purkinje cells (39; Fig. 5*K*), in the present study in PLCβ4-deficient mice, DHPG did not induce Ca^{2+} mobilization ($n = 3$; Fig. 5, *C* and *E*) in *lobe 6* Purkinje cells but increased dendritic $[Ca^{2+}]_i$ to a small degree in *lobe 9* Purkinje cells ($n = 4$; Fig. 5, *H* and *J*). To exclude the possibility that the lack of Ca^{2+} release in the mutant mice was an artifact of slice preparation, we examined AMPAR-induced Ca^{2+} release after DHPG stimulation. Application of AMPA evoked a large Ca^{2+} transient in Purkinje cells in wild-type cerebellum (Fig. 5*K*). As shown in Fig. 5 (*E* and *J*), large Ca^{2+} responses were also obtained in Purkinje cells in rostral and caudal cerebellum from PLCβ4-deficient mice following application of AMPA. There was an additional slow phase of the AMPA-induced Ca^{2+} response in the dendrite (Fig. 5, *E*, *J*, and *K*), which may be due to Ca^{2+} signals traveling from distal parts of the dendrite. In the soma, however, the two phases overlapped. These results suggest that classic PKC isozymes were not activated in rostral cerebellum from PLCβ4-deficient mice.

To investigate possible colocalization of classic PKC isozymes with PLCβ4, we examined the distribution of classic PKC isozymes using antibodies against each isozyme. Immunostaining with antibodies were done as described under "Experimental Procedure." As shown in Fig. 6 (*A–D*), PKCα, βI, and γ were expressed uniformly in Purkinje cells, whereas PKCβII was not detected. These data are consistent with data obtained previously by several authors (23, 25). To investigate the PKC isozymes coupled to PLCβ4 and PLCβ3, we examined the translocation of PKC isozymes during LTD induction using immunohistochemistry. Fluorescence-labeled secondary antibodies were used in this experiment, because fluorescent images showed a relatively large difference between wild-type and PLCβ4-deficient mice with high contrast. 400-μm cerebellar slices from wild-type ($n = 8$ from four mice) and PLCβ4-deficient mice ($n = 8$ from four mice) were incubated for 5 min in ACSF with ($n = 4$ of each mice) or without ($n = 4$ of each mice) 100 μM glutamate and 50 mM KCl. After stimulation, samples were rinsed for 5 min, followed by fixation. From 10 to 15 sections (5-μm thickness) from each slice were stained with antibodies. In wild-type mice, there was strong staining for PKCα in the dendrites of Purkinje cells (Fig. 6*F*), indicating that PKCα is translocated. In contrast, no stain was detected in dendrites in PLCβ4-deficient mice (Fig. 6*G*). PKCβI immunoreactivity was very strong in Purkinje cell dendrites and soma in all lobes of wild-type mice (Fig. 6*I*), whereas the fluorescent signal was observed only in cell somas in rostral part of PLCβ4-deficient mice (Fig. 6*J*). No difference in staining for PKCγ, however, was detectable between wild-type and PLCβ4-deficient mice (Fig. 6, *L* and *M*).

Unfortunately, we could not determine the coupling selectivity between PLC (β3 and β4) and PKC (α and βI), because imaging of PKC in caudal part is not clear (data not shown). To overcome this difficulty, a real time imaging of GFP-labeled PKC in living cells under LTD condition is desirable, but it is impossible at present stage. Therefore, we concluded that, at the lowest estimate, both PKCα and PKCβI were translocated during LTD induction, but PKCγ was not.

DISCUSSION

In the present study, the mGluR1-mediated Ca^{2+} response and LTD induction was greatly reduced in the rostral cerebellum from PLCβ4-deficient mice, an area in which PLCβ1 and PLCβ3 were also not expressed strongly in these mutant mice. In the caudal cerebellum, however, the residual PLCβ3 activity was sufficient to generate Ca^{2+} elevation and LTD induction. These results suggest that there was a minimum level of PLCβ3 and PLCβ4 required to generate the mGluR1-mediated Ca^{2+} response and LTD. We also showed that LTD induction in rostral and caudal cerebellum required activation of classic PKC isozymes.

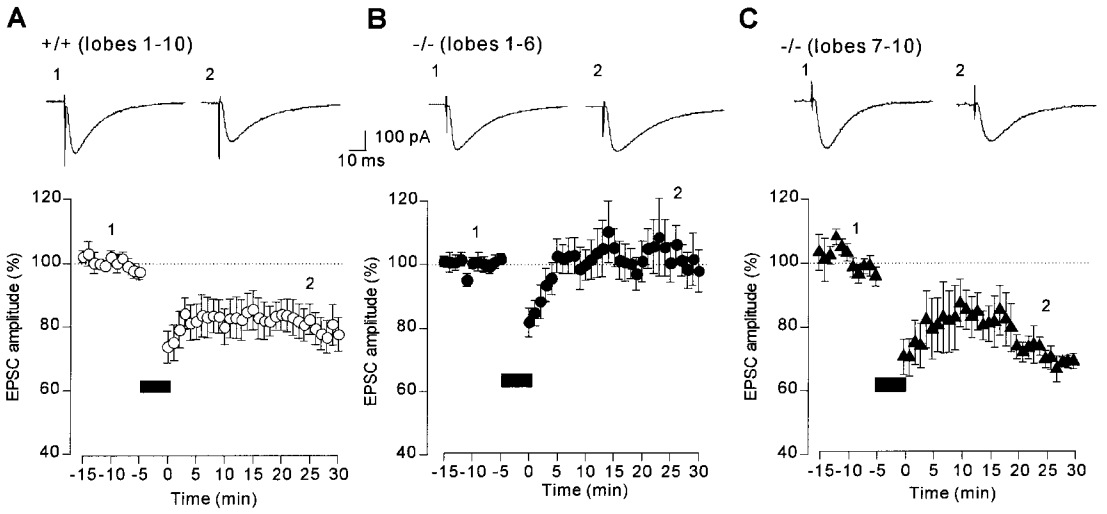

FIG. 4. **LTD of PF-EPSCs was impaired in the rostral cerebellum from PLCβ4-deficient mice.** The amplitude of PF-EPSCs in Purkinje cells from wild-type (*A*) and PLCβ4-deficient (*B* and *C*) mice. Cerebellar LTD in PLCβ4-deficient mice was impaired in the rostral cerebellum (*lobes 1–6*; *B*), whereas LTD in the caudal cerebellum (*lobes 7–10*; *C*) was not different from that observed in wild-type mice. The EPSC was evoked by stimulation of PF at 0.2 Hz throughout the experiments. Depolarization to +20 mV for 200 ms was applied 300 times in conjunction with PF stimulation (CJ) over 5 min as indicated by the *bar*. *Traces* are averages of 10 individual EPSCs recorded before (*1*) and 25 min after (*2*) CJ stimulation. Data points represent the mean ± S.E.

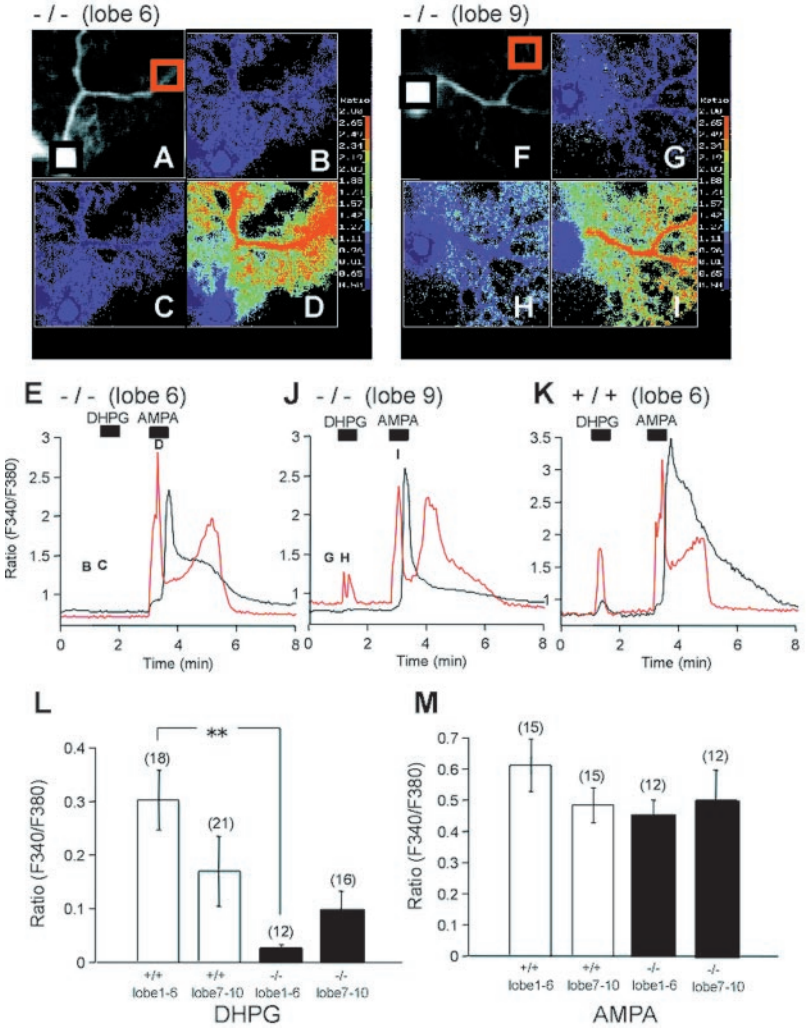

FIG. 5. **Lack of DHPG-induced Ca^{2+} mobilization in Purkinje cells of rostral cerebellum of PLCβ4-deficient mice.** *A* and *F*, representative fluorescence images (380-nm excitation wavelength) before application of DHPG. The *red* and *black boxes* indicate the position where the Ca^{2+} level was measured in the dendrites and soma, respectively. Pseudocolor ratio images at the time indicated (*B–D*, *G–I*). The time course of changes in F_{340}/F_{380} ratio (*E*, *J*, and *K*). The application of DHPG (30 μM, 30 s) did not induce an increase in $[Ca^{2+}]_i$ in Purkinje cells in *lobe 6*, whereas a small rise was observed in *lobe 9* from PLCβ4-deficient mice. Purkinje cells were voltage-clamped at a holding potential of −60 mV. Changes in $[Ca^{2+}]_i$ in response to an application of AMPA (10 μM, 30 s) were unaltered. Both DHPG and AMPA produced Ca^{2+} elevations in Purkinje cells in *lobe 6* from wild-type mice (*K*). *L* and *M*, average F_{340}/F_{380} values during stimulation with DHPG (*L*) or AMPA (*M*) in Purkinje cells from wild-type and PLCβ4-deficient mice. Fluorescence of Purkinje cells in cerebellar slices loaded with fura-2 AM was recorded in the presence of tetrodotoxin (0.5 μM). The *numbers in parentheses* indicate the number of Purkinje cells tested. *Bars* represent mean ± S.E. **, $p < 0.01$.

Differential Functional Localization of PLCβ Isoforms and Intracellular Ca^{2+} Elevation—We used immunohistochemical and Western blot analyses to localize the PLCβ isoforms in the wild-type mouse cerebellum: PLCβ1 was expressed uniformly and weakly, PLCβ2 was not detected, PLCβ3 was expressed predominantly in caudal cerebellar Purkinje cells (*lobes 7–10*), and PLCβ4 was expressed uniformly and strongly throughout cerebellar Purkinje cells. These results are consistent with

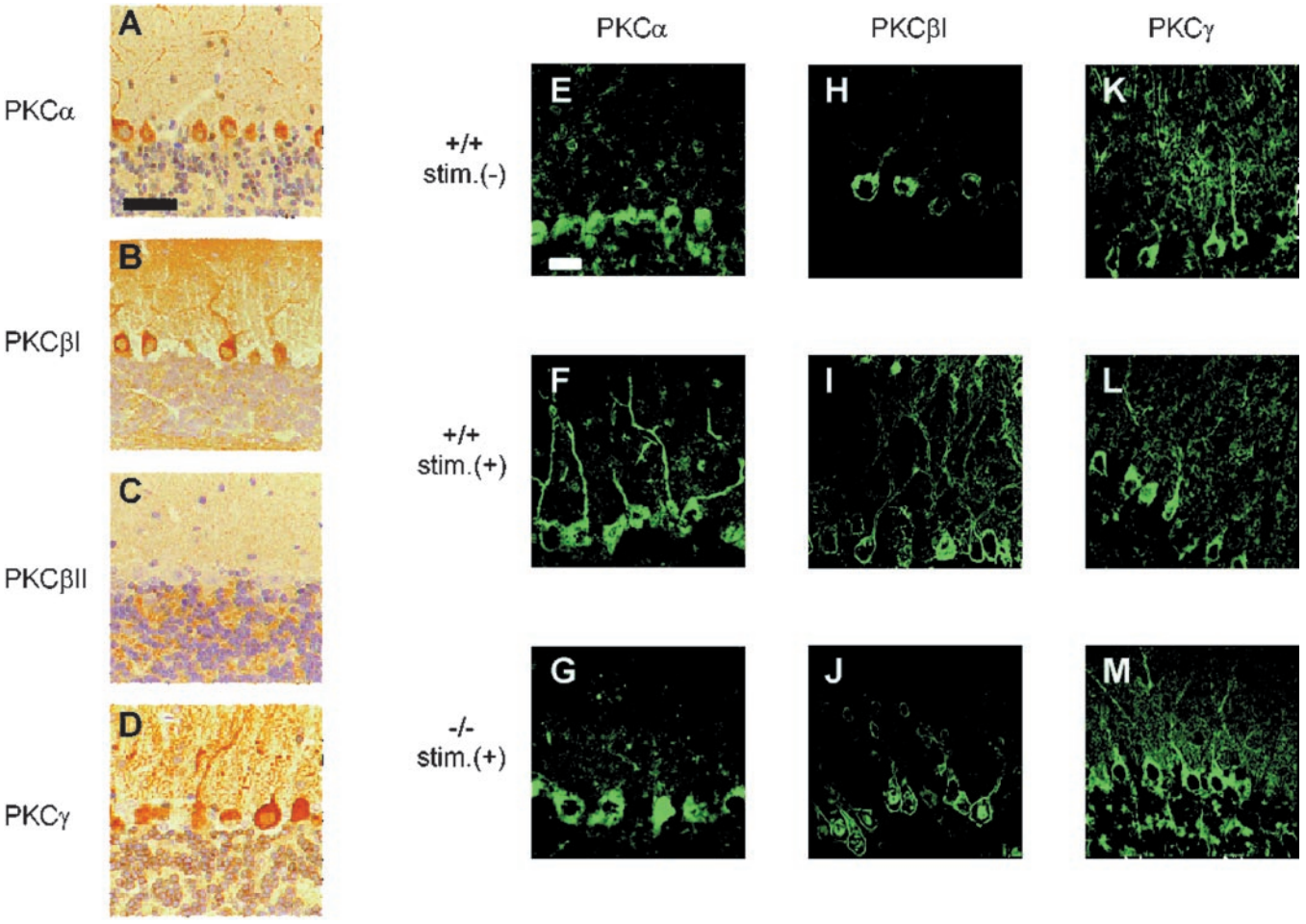

FIG. 6. **Localization of PKC isozymes in Purkinje cells after application of the LTD-inducing stimulation paradigm.** Cerebellar sections from wild-type mice were immunostained with anti-PKCα (*A*), -βI (*B*), -βII (*C*), or -γ (*D*) antibodies. Purkinje cells exhibited intense and uniform PKCα, -βI, and -γ immunoreactivity. PKCβII was present only in the granule cell layer. Fluorescence images show PKC isozymes after LTD induction in rostral cerebellum. Unstimulated (*stim.(-)*; *E*, *H*, and *K*) and stimulated (*stim.(+)*; *F*, *G*, *I*, *J*, *L*, *M*) cerebellar slices were stained with anti-PKCα (*E–G*), anti-PKCβI (*H–J*), or anti-PKCγ antibody (*K–M*). PKCα immunoreactivity appeared in Purkinje cell dendrites and soma in wild-type (+/+) mice 5 min after stimulation (*F*), whereas only cell somas were stained in PLCβ4-deficient (−/−) mice (*G*). PKCβI immunoreactivity was observed in Purkinje cell dendrites in wild-type (+/+) mice (*I*) with LTD stimulation, whereas no immunoreactivity was observed in dendrites in PLCβ4-deficient (−/−) mice (*J*). Fluorescence images of Purkinje cells were not different between wild-type (*L*) and PLCβ4-deficient mice (*M*) when using anti-PKCγ antibody. *Bar* = 100 μm in *A–D* and 50 μm in *E–M*.

previous reports of expression of the corresponding PLCβ isoform mRNA (11–13). In PLCβ4-deficient mice, Although PLCβ1 was expressed in rostral cerebellar Purkinje cells, Purkinje cells in rostral cerebellum from PLCβ4-deficient mice lacked the mGluR1-mediated Ca^{2+} response. These results indicate that (i) PLCβ1 is not involved in the mGluR1-mediated signaling pathway in cerebellar Purkinje cells and does not have a role in the induction of cerebellar LTD and (ii) mGluR1-mediated responses in caudal cerebellar Purkinje cells from PLCβ4-deficient mice were produced by activation of PLCβ3 alone. These results suggest that PLCβ4 is a link between the activation of mGluR1 and the induction of LTD in rostral cerebellar Purkinje cells.

Involvement of PKC Isozymes in the Formation of LTD—The results of the present study showing that LTD induction was greatly reduced in PLCβ4-deficient mice is consistent with the lack of LTD in cerebellum from mGluR1-deficient mice (6, 7) but does not appear to be consistent with the intact LTD induction observed in PKCγ-deficient mice (8) if PLCβ4 activates PKCγ. Recent evidence using the expression of a PKC inhibitor in Purkinje cells indicates that PKC is required for LTD induction (26). PKCα, βI, and γ were expressed strongly and uniformly in cerebellar Purkinje cells, whereas PKCβII was not expressed in Purkinje cells as shown in Fig. 6 (*A–D*) (25). PKCδ, ϵ, and ζ were also expressed in cerebellar Purkinje cells (23); however, these isozymes are Ca^{2+}-independent (for review, see Ref. 38), thus, the contribution of these isozymes to LTD induction is likely to be small. Therefore, the remaining isozymes, PKCα and/or PKCβI, may compensate for the lack of PKCγ in rostral cerebellum of PKCγ-deficient mice.

In PLCβ4-deficient mice, there did not appear to be any compensation for the lack of PLCβ4 by PLCβ1 in the rostral cerebellum. Thus, evidence suggests that, although compensation for deletion of protein isoforms in the signaling pathway downstream of PLCβ occurs, there is no compensatory mechanism for the deletion of PLCβ4 itself.

Select PKC Translocation during LTD Induction—Translocation of PKC isozymes after 12-*O*-tetradecanoylphorbol-13-acetate (TPA) stimulation has been clearly observed in several cell systems (40–44) but not with stimulation sufficient for LTD induction. As described above, the combination of PLC (β3 and β4) activation and translocation of PKC (α and βI) is very likely. Translocation of PKCγ has been observed after stimulation used to induce long term potentiation in neurons in the CA1 region of hippocampus (45, 46) and TPA stimulation in COS-7 cells (43) but not by LTD-forming conditions in Purkinje cells in the present study. This is consistent with previous results from PKCγ-deficient mice (8). This result further indi-

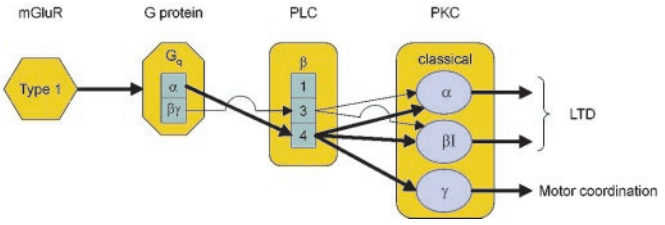

FIG. 7. **Model of the mGluR1 signaling pathway involved in cerebellar LTD induction and eye blink conditioning.** PLCβ4, PKCα, and PKCβI have major roles in LTD induction in rostral cerebellum.

cates that PKCγ was not activated by the signaling pathway through PLCβ3 and PLCβ4 in cerebellar Purkinje cells.

It has been reported that Purkinje cells in rostral cerebellum from PLCβ4-deficient mice form persistent multiple synapses with climbing fibers (19). This difference may underlie the lack of LTD induction in PLCβ4-deficient mice, however, Chen *et al.* (8) report that, in PKCγ-deficient mice also, each climbing fiber forms multiple synapses with Purkinje cells and generates multiple spikes that resemble complex spikes, and these mice do exhibit LTD. Thus, the persistent multiple innervation of Purkinje cells by climbing fibers in rostral cerebellum of PLCβ4-deficient mice does not appear to be involved in LTD induction. Moreover, eye blink conditioning is impaired in PLCβ4-deficient mice (47). The results from the present study support the idea that induction of LTD has a role in eye blink conditioning, but the developmental shift from multiple to mono-innervation of Purkinje cells by climbing fibers does not have a role in either LTD induction or eye blink conditioning. These ideas are expressed in Fig. 7 as a molecular linkage of mGluR1-G_q-PLCβ4-PKCα and/or PKCβI.

Taken together, the results obtained in the present study provide strong support for the idea that cerebellar LTD involves PKC activation. Further studies are needed to determine if the signaling pathway involves more specific combinations between signaling molecules, such as mGluR1-G_q-PLCβ4-PKCα or mGluR1-G_q-PLCβ3-PKCβI.

Acknowledgments—We thank S. Konishi, A. Aiba, K. Nakamura, and H. Kojima for their expert technical advice, and C. N. Allen for critically reading the manuscript.

REFERENCES

1. Ito, M., Sakurai, M., and Tongroach, P. (1982) *J. Physiol.* **324,** 113–134
2. Ekerot, C. F., and Kano, M. (1985) *Brain Res.* **342,** 357–360
3. Sakurai, M. (1987) *J. Physiol.* **394,** 463–480
4. Kim, J. J., and Thompson, R. F. (1997) *Trends Neurosci.* **20,** 177–181
5. Linden, D. J., and Connor, J. A. (1995) *Annu. Rev. Neurosci.* **18,** 319–357
6. Aiba, A., Kano, M., Chen, C., Stanton, M. E., Fox, G. D., Herrup, K., Zwingman, T. A., and Tonegawa, S. (1994) *Cell* **79,** 377–388
7. Conquet, F., Bashir, Z. I., Davies, C. H., Daniel, H., Ferraguti, F., Bordi, F., Franz-Bacon, K., Reggiani, A., Matarese, V., and Conde, F. (1994) *Nature* **372,** 237–243
8. Chen, C., Kano, M., Abeliovich, A., Chen, L., Bao, S., Kim, J. J., Hashimoto, K., Thompson, R. F., and Tonegawa, S. (1995) *Cell* **83,** 1233–1242
9. Cockcroft, S., and Thomas, G. M. (1992) *Biochem. J.* **288,** 1–14
10. Rhee, S. G., and Bae, Y. S. (1997) *J. Biol. Chem.* **272,** 15045–15048
11. Tanaka, O., and Kondo, H. (1994) *Neurosci. Lett.* **182,** 17–20
12. Roustan, P., Abitbol, M., Menini, C., Ribeaudeau, F., Gerard, M., Vekemans, M., Mallet, J., and Dufier, J. L. (1995) *Neuroreport* **6,** 1837–1841
13. Watanabe, M., Nakamura, M., Sato, K., Kano, M., Simon, M. I., and Inoue, Y. (1998) *Eur. J. Neurosci.* **10,** 2016–2025
14. Yoshioka, T., Inoue, H., Kasama, T., Seyama, Y., Nakashima, S., Nozawa, Y., and Hotta, Y. (1985) *J. Biochem.* (*Tokyo*) **98,** 657–662
15. Kim, M. J., Bahk, Y. Y., Min, D. S., Lee, S. J., Ryu, S. H., and Suh, P. G. (1993) *Biochem. Biophys. Res. Commun.* **194,** 706–712
16. Jiang, H., Lyubarsky, A., Dodd, R., Vardi, N., Pugh, E., Baylor, D., Simon, M. I., and Wu, D. (1996) *Proc. Natl. Acad. Sci. U. S. A.* **93,** 14598–14601
17. Kim, D., Jun, K. S., Lee, S. B., Kang, N. G., Min, D. S., Kim, Y. H., Ryu, S. H., Suh, P. G., and Shin, H. S. (1997) *Nature* **389,** 290–293
18. Shibuki, K., Gomi, H., Chen, L., Bao, S., Kim, J. J., Wakatsuki, H., Fujisaki, T., Fujimoto, K., Katoh, A., Ikeda, T., Chen, C., Thompson, R. F., and Itohara, S. (1996) *Neuron* **16,** 587–599
19. Kano, M., Hashimoto, K., Watanabe, M., Kurihara, H., Offermanns, S., Jiang, H., Wu, Y., Jun, K., Shin, H. S., Inoue, Y., Simon, M. I., and Wu, D. (1998) *Proc. Natl. Acad. Sci. U. S. A.* **95,** 15724–15729
20. Kano, M., Hashimoto, K., Kurihara, H., Watanabe, M., Inoue, Y., Aiba, A., and Tonegawa, S. (1997) *Neuron* **18,** 71–79
21. Kashiwabuchi, N., Ikeda, K., Araki, K., Hirano, T., Shibuki, K., Takayama, C., Inoue, Y., Kutsuwada, T., Yagi, T., and Kang, Y. (1995) *Cell* **81,** 245–252
22. Kano, M., Hashimoto, K., Chen, C., Abeliovich, A., Aiba, A., Kurihara, H., Watanabe, M., Inoue, Y., and Tonegawa, S. (1995) *Cell* **83,** 1223–1231
23. Wetsel, W. C., Khan, W. A., Merchenthaler, I., Rivera, H., Halpern, A. E., Phung, H. M., Negro-Vilar, A., and Hannun, Y. A. (1992) *J. Cell Biol.* **117,** 121–133
24. Chen, S., and Hillman, D. E. (1993) *Neuroscience* **56,** 177–188
25. Garcia, M. M., and Harlan, R. E. (1997) *J. Comp. Neurol.* **385,** 26–42
26. De Zeeuw, C. I., Hansel, C., Bian, F., Koekkoek, S. K., van Alphen, A. M., Linden, D. J., and Oberdick, J. (1998) *Neuron* **20,** 495–508
27. Capecchi, M. R. (1989) *Science* **244,** 1288–1292
28. Nakao, K., Nakagata, N., and Katsuki, M. (1998) *Exp. Anim.* (*Tokyo*) **47,** 167–171
29. Min, D. S., Kim, D. M., Lee, Y. H., Seo, J., Suh, P. G., and Ryu, S. H. (1993) *J. Biol. Chem.* **268,** 12207–12212
30. Guesdon, J. L., Ternynck, T., and Avrameas, S. (1979) *J. Histochem. Cytochem.* **27,** 1131–1139
31. Warnke, R., and Levy, R. (1980) *J. Histochem. Cytochem.* **28,** 771–776
32. Nakazawa, K., Mikawa, S., Hashikawa, T., and Ito, M. (1995) *Neuron* **15,** 697–709
33. Murashima, M., and Hirano, T. (1999) *J. Neurosci.* **19,** 7326–7333
34. Llano, I., Marty, A., Armstrong, C. M., and Konnerth, A. (1991) *J. Physiol.* **434,** 183–213
35. Konnerth, A., Llano, I., and Armstrong, C. M. (1990) *Proc. Natl. Acad. Sci. U. S. A.* **87,** 2662–2665
36. Crepel, F., and Krupa, M. (1988) *Brain Res.* **458,** 397–401
37. Hirano, T. (1990) *Neurosci. Lett.* **119,** 145–147
38. Nishizuka, Y. (1995) *FASEB J.* **9,** 484–496
39. Netzeband, J. G., Parsons, K. L., Sweeney, D. D., and Gruol, D. L. (1997) *J. Neurophysiol.* **78,** 63–75
40. Staak, S., Behnisch, T., and Angenstein, F. (1995) *Brain Res.* **682,** 55–62
41. Sena, C. M., Rosario, L. M., Parker, P. J., Patel, V., and Boarder, M. R. (1996) *J. Neurochem.* **66,** 1086–1094
42. Son, H., Madelian, V., and Carpenter, D. O. (1996) *Brain Res.* **739,** 282–292
43. Sakai, N., Sasaki, K., Ikegaki, N., Shirai, Y., Ono, Y., and Saito, N. (1997) *J. Cell Biol.* **139,** 1465–1476
44. Buchner, K., Adamec, E., Beermann, M. L., and Nixon, R. A. (1999) *Brain Res. Mol. Brain Res.* **64,** 222–235
45. Van der Zee, E. A., Luiten, P. G., and Disterhoft, J. F. (1997) *Prog. Neuropsychopharmacol. Biol. Psychiatry* **21,** 531–572
46. Angenstein, F., Riedel, G., Reyman, K. G., and Staak, S. (1999) *Neuroscience* **93,** 1289–1295
47. Kishimoto, Y., Hirono, M., Sugiyama, T., Kawahara, S., Nakao, K., Kishio, M., Katsuki, M., Yoshioka, T., and Kirino, Y. (2001) *Neuroreport*, in press

Phospholipase Cβ4 and Protein Kinase Cα and/or Protein Kinase CβI Are Involved in the Induction of Long Term Depression in Cerebellar Purkinje Cells

Moritoshi Hirono, Takashi Sugiyama, Yasushi Kishimoto, Ikuko Sakai, Takahito Miyazawa, Masahiro Kishio, Hiroko Inoue, Kazuki Nakao, Masayuki Ikeda, Shigenori Kawahara, Yutaka Kirino, Motoya Katsuki, Hidenori Horie, Yoshihiro Ishikawa and Tohru Yoshioka

J. Biol. Chem. 2001, 276:45236-45242.
doi: 10.1074/jbc.M105413200 originally published online September 10, 2001
